Journal of Organometallic Chemistry 694 (2009) 2463–2466

Contents lists available at ScienceDirect

Journal of Organometallic Chemistry

journal homepage: www.elsevier.com/locate/jorganchem

Note

New examples of mixed organochalcogene compounds: Synthesis, structural features and spectroscopic data of [PhSe(etu)][PhTeX$_4$] (Ph = phenyl; etu = ethylenethiourea; X = Br, I)

Gelson Manzoni de Oliveira [a,*], Gleison Antônio Casagrande [b], Ernesto Schulz Lang [a,*], Rozanna Marques Muzzi [b], Sebastião de Souza Lemos [c]

[a] *Departamento de Química, Laboratório de Materiais Inorgânicos, Universidade Federal de Santa Maria – UFSM, 97115-900 Santa Maria, RS, Brazil*
[b] *Faculdade de Ciências Exatas e Tecnologia, Universidade Federal da Grande Dourados – UFGD, 79804-970 Dourados, MS, Brazil*
[c] *Instituto de Química, Campus Darcy Ribeiro, Universidade de Brasília – UnB, 70904-970 Brasília, DF, Brazil*

ARTICLE INFO

Article history:
Received 5 March 2009
Received in revised form 7 April 2009
Accepted 7 April 2009
Available online 17 April 2009

Keywords:
Organochalcogene compounds
Mixed-valent arylchalcogenyl halides
Organyltellurenyl halides
Secondary interactions

ABSTRACT

(PhSe)$_2$ reacts with Br$_2$, ethylenethiourea and PhTeBr$_3$, further with I$_2$, ethylenethiourea and PhTeI$_3$, to give [PhSe(etu)][PhTeBr$_4$] (**1**) (Ph = phenyl; etu = ethylenethiourea) and [PhSe(etu)][PhTeI$_4$] (**2**) in very good yields.

The tellurium centers present a distorted octahedral configuration, achieved through dimerization involving secondary, reciprocal Te···X interactions.

In both compounds the anionic dimmers are linked through X···X interactions, attaining a one-dimensional, polymeric assembly along the *b* axis. Cations and anions are linked through short Se···X contacts. In addition to single crystal X-ray data, multinuclear NMR results for **1** and **2** are also presented and discussed.

1. Introduction

Structural aspects of organochalcogene compounds with mixed valences have been discussed by Hauge [1], Pathirana [2] and co-workers and represent only one of different and interesting facets of a kind of compounds which overpass simple description, so that concepts like hypervalence, multicenter bonding, charge transfer interactions, secondary bonding, have been introduced to describe their structural and chemical properties [3,4].

Organyltellurenyl(IV) halides such as [ArTeX$_4$]$^-$ (X = Cl, Br, I) in form of polymeric chains or oligomeric structures, stabilized with a wide range of counter ions such as protonated amines, alkali metal cations, etc. are well known [5–8]. Most of these complex salts lie close to the ionic/covalent borderline and show properties of supramolecules due to interionic, fairly strong secondary bonds of the types N$^+$–H···Te, Te···X or X···X (X = Cl, Br, I), as well as Te···π-aryl contacts [9,10]. Polymeric structures with the chalcogen atoms presenting mixed valence states, like for example the neutral species [mesTeI(μ-I)$_2$(TeImes)$_2$]$_n$ [11], appear rarely in the literature. Also unusual are mixed-valent complex salts of different chalcogene atoms with the oxidation states +2 and +4 for the cation and the anion, respectively [12,13]. Recently, Beckmann and co-workers [14] have discussed the synthesis of the very uncommon mixed-valent aryltellurenyl halides RX$_2$TeTeR (X = Cl, Br; R = Ph, 2,6-Mes$_2$C$_6$H$_3$; Mes = 2,4,6-Me$_3$C$_6$H$_2$), with vicinal, asymmetrically substituted tellurium atoms with the oxidation numbers +1 and +3.

In the light of our experimental interests, we report in this communication the synthesis and the structural characterization of the polymeric, mixed-valent complex salts of selenium^{II} and tellurium^{IV} [PhSe(etu)][PhTeX$_4$] (Ph = phenyl; etu = ethylenethiourea; X = Br, I). In both compounds the tellurium atoms present a distorted octahedral geometry, achieved by dimerization through interionic, secondary Te···X interactions. These interactions support also the polymeric, one-dimensional assembly of the lattices of the new compounds.

2. Results and discussion

2.1. X-ray structures of crystals 1 and 2

The X-ray crystal data and the experimental conditions for the analyses of the complexes [PhSe(etu)][PhTeBr$_4$] (**1**) and [PhSe(etu)][PhTeI$_4$] (**2**) are given in Table 1. Table 2 resumes selected bond distances and angles for the title complexes. Fig. 1 shows the asymmetric unit and the dimerization of the compound **1**, with the secondary interactions identified by dashed lines.

---

* Corresponding authors. Tel.: +55 55 3220 8980; fax: +55 55 3220 8031.
E-mail addresses: manzonideo@smail.ufsm.br (G. Manzoni de Oliveira), eslang@smail.ufsm.br (E. Schulz Lang).

0022-328X/$ - see front matter © 2009 Elsevier B.V. All rights reserved.
doi:10.1016/j.jorganchem.2009.04.009

Table 1
Crystal data and structure refinement for **1** and **2**.

	1	**2**
Empirical formula	$C_{15}H_{16}Br_4N_2SSeTe$	$C_{15}H_{16}I_4N_2SSeTe$
Formula weight	782.56	970.52
T (K)	296(2)	296(2)
Radiation, λ (Å)	Mo Kα, 0.71073	Mo Kα, 0.71073
Crystal system, space group	triclinic, $p\bar{1}$	triclinic, $p\bar{1}$
Unit cell dimensions		
a (Å)	9.256(1)	9.505(1)
b (Å)	9.335(1)	9.662(1)
c (Å)	13.189(1)	13.638(1)
α (°)	96.19(1)	83.69(1)
β (°)	91.29(1)	89.41(1)
γ (°)	103.90(1)	76.75(1)
Volume (Å^3)	1098.39(19)	1211.6(2)
Z, Calculated Density (g cm^{-3})	2, 2.366	2, 2.660
Absorption coefficient (mm^{-1})	10.383	7.914
F(0 0 0)	724	868
Crystal size (mm)	0.1 × 0.15 × 0.1	0.1 × 0.1 × 0.1
θ Range (°)	2.79–25.50	2.65–26.01
Index ranges	$-11 \leqslant h \geqslant 11$, $-11 \leqslant k \geqslant 11$, $-15 \leqslant l \geqslant 15$	$-11 \leqslant h \geqslant 11$, $-11 \leqslant k \geqslant 11$, $-16 \leqslant l \geqslant 16$
Reflections collected	8260	10 920
Reflections unique	4061 [$R_{int} = 0.0748$]	4691 [$R_{int} = 0.0830$]
Completeness to theta max.	99.2%	98.3%
Absorption correction	analytical	analytical
Max. and min. transmission	0.4043 and 0.0938	0.7033 and 0.4322
Refinement method	full-matrix least-squares on F^2	Full-matrix least-squares on F^2
Data/restraints/parameters	4061/0/217	4691/0/194
Goodness-of-fit (GOF) on F^2	1.001	1.097
Final R indices [$I > 2\sigma(I)$]	$R_1 = 0.0480$, w$R_2 = 0.1136$	$R_1 = 0.0997$, w$R_2 = 0.2470$
R indices (all data)	$R_1 = 0.0812$, w$R_2 = 0.1325$	$R_1 = 0.1298$, w$R_2 = 0.2588$
Largest diff. peak and hole (e Å^{-3})	0.745 and 1.186	2.536 and 1.484

Complex **2** shows the same structural and dimeric configuration as compound **1**, since both compounds **1** and **2** are isomorphous. Fig. 2 presents the one-dimensional assembly of compound **2** along the b axis, attained through secondary I···I interactions. The one-dimensional polymerization of the dimers in complex **1** is achieved through Br···Br interactions.

In [PhSe(etu)][PhTeBr$_4$] (**1**), the Br1···Te secondary interactions have a distance of 3.7598(4) Å, quite longer than the covalent Te–Br mean distance, 2.69 Å. In [PhSe(etu)][PhTeI$_4$] (**2**) the I3···Te1 secondary interactions measure 3.803(3) Å and the covalent Te–I mean distance is 2.94 Å. The polymeric assembly of **1** and **2** along the b axis occurs through secondary Br···Br {3.7957(17)} and I···I {3.813(3) Å} interactions. The octahedral axis C11–Te···Br1#1 in **1**

Table 2
Selected bond lengths [Å] and angles [°] for **1** and **2**.

1		**2**	
Bond lengths			
C11–Te	2.141(6)	C11–Te1	2.153(12)
C21–Se	1.925(8)	C21–Se	1.880(16)
Br1–Te	2.7444(10)	Te1–I1	2.893(3)
Br2–Te	2.6843(11)	Te1–I2	2.917(2)
Br3–Te	2.65585(10)	Te1–I4	2.941(3)
Br4–Te	2.6869(12)	Te1–I3	3.000(3)
S–Se	2.2253(3)	Te1···I3#1	3.803(3)
Se···Br3	3.2857(4)	Se–S	2.233(9)
Te···Br1#1	3.7598(4)	I4···I2#3	3.813(3)
Bond angles			
Te–Br1···Te#1	98.731(2)	C11–Te1–I1	91.6(5)
Br1–Te···Br#1	81.269(3)	C11–Te1–I2	90.3(5)
S–Se···Br3	165.88(5)	I1–Te1–I2	91.75(7)
Se···Br3–Te	97.432(4)	C11–Te1–I4	88.9(5)
C1–S–Se	101.9(3)	I1–Te1–I4	88.53(8)
C21–Se–S	99.7(2)	I2–Te1–I4	179.20(8)
C11–Te–Br3	90.15(2)	C11–Te1–I3	91.2(5)
C11–Te–Br2	88.4(2)	I1–Te1–I3	176.22(9)
Br3–Te–Br2	92.12(3)	I2–Te1–I3	90.72(7)
C11–Te–Br4	88.0(2)	I4–Te1–I3	89.05(8)
Br3–Te–Br4	88.77(4)	C21–Se–S	98.2(8)
Br2–Te–Br4	176.33(3)	C11–Te1···I3#1	170.9(5)
C11–Te–Br1	89.6(2)	Te1–I3···Te1#1	98.023(6)
Br3–Te–Br1	177.28(4)	Te1–I4···I2#2	174.82(8)
Br2–Te–Br1	90.58(3)	Te1–I2···I4#2	175.19(8)
Br4–Te–Br1	88.52(4)	I3–Te1···I3#1	81.977(6)
C11–Te···Br1#1	166.184(4)	C11–Te1···I3#1	170.875(4)

Symmetry transformations used to generate equivalent atoms: **1**{#1: $-x + 2$, $-y + 2$, $-z$}; **2**{#1: $-x$, $-y + 2$, $-z$; #2: x, $1 + y$, z; #3: $-x$, $-y + 3$, $-z$}.

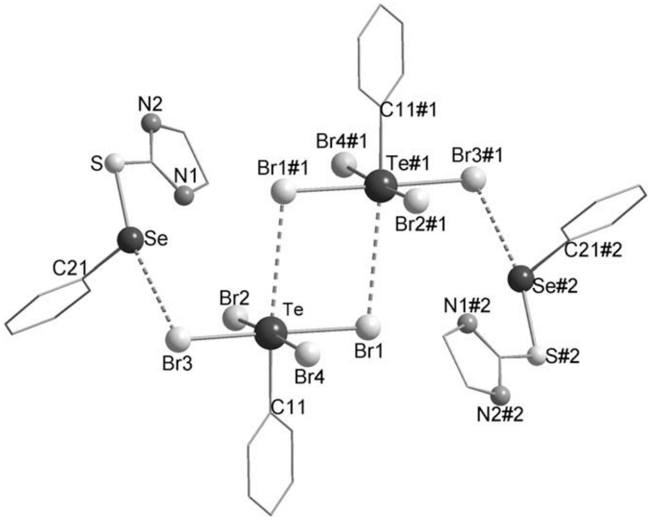

Fig. 1. Molecular structure and dimeric configuration of [PhSe(etu)][PhTeBr$_4$] (**1**). Interionic, secondary interactions are depicted in dashed lines. Symmetry transformations used to generate equivalent atoms: #1: $-x + 2$, $-y + 2$, $-z$; #2: $-x + 1$, $-y + 1$, $-z$.

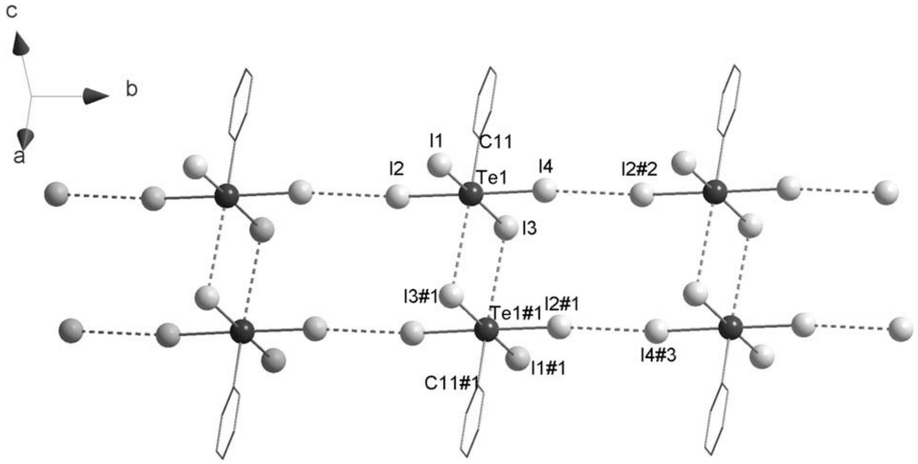

Fig. 2. One-dimensional assembly of the dimers $[PhTeI_4]_2^{2-}$ of **2** along the *b* axis. For clarity the cations $[PhSe(etu)]^+$ are not shown. Dashed lines represent secondary interactions. Symmetry transformations used to generate equivalent atoms: #1: $-x$, $-y+2$, $-z$; #2: x, $y+1$, z; #3: $-x$, $-y+3$, $-z$.

presents an angle of 166.184(4)° and in **2** the equivalent axis C11–Te1···I3#1 is somewhat open, with 170.875(4)°.

Interesting details in the structures of **1** and **2** are the small distances of the cation–anion Se···Br and Se···I interactions, respectively 3.2857(4) and 3.412(5) Å, which are remarkable shorter than the sum of the Se/Br and Se/I van der Waals radii, 3.75 and 3.88 Å [15], respectively. Interactions of the same type described in analogue compounds [12] are rather longer, like for example, Se···Br = 3.7113(18) and Se···I = 3.9485(12) Å. The shorter Se···Br and Se···I distances in **1** and **2** could suggest a molecular representation for both compounds, such us $[Ph(etu)Se(\mu\text{-}X)TeX_3Ph]$.

However, the ionic formulation of compounds $[PhSe(etu)][PhTeBr_4]$ (**1**) and $[PhSe(etu)][PhTeI_4]$ (**2**) is strongly supported by the fact that the Se···Br and Se···I interactions, although uncommonly shorter, are much longer than analogue bond lengths of related structures previously reported, for examples, Se···Br = 2.3331(8) Å [16,17] and Se···I = 2.564(1), 2.720(1) Å [18,19].

Finally, a chlorine compound similar to **1** and **2** could not be attained, since the instability of the Te–Cl bond leads to hydrolysis of $PhTeCl_3$ (see Section 3), with formation of PhTe(O)OH (arene tellurinic anhydride) [20].

2.2. ^{77}Se and ^{125}Te NMR data

Attempts to study the dissociation of the title complexes in solution by means of multinuclear NMR spectra were limited by the fact that the crystals of **1** and **2** are soluble only in polar or coordinating solvents like acetone or dimethylsulfoxide (DMSO). ^{1}H, ^{13}C, ^{77}Se and ^{125}Te NMR measures were conducted in solutions of acetone-d_6 and DMSO-d_6 in a 9:1 proportion, respectively. Since compounds **1** and **2** do not show many significant features in their ^{1}H or ^{13}C NMR spectra, our attention was turned to the ^{77}Se and ^{125}Te NMR spectroscopy. Complex **1** generates one lone sharp peak in the ^{77}Se NMR spectrum, localized in 292.8 ppm, and two near signals for ^{125}Te NMR: an intensive peak at 1201.8 ppm and a smaller signal at 1189.2 ppm, both keeping a proportion of about 5.5:1. The lone peak in the ^{77}Se NMR spectrum of **1** (292.8 ppm) indicates the occurrence of one single Se species, very possibly the cation $[PhSe(etu)]^+$. The species $[PhTeBr_4]^-$ should explain the strong signal appearing at 1201.8 ppm in the ^{125}Te NMR spectrum of **1**; the partial decomposition of this main product would explain the small signal localized in 1189.2 ppm.

In the ^{77}Se NMR spectrum of complex **2** there are two signals, at 684.9 and 292.7 ppm, in a relation of approximately 1:3, respectively. These two ^{77}Se NMR signals of **2** indicate the occurrence of a second Se species in solution, possibly attained by coordination of the ion $[PhSe(etu)]^+$ with solvent molecules after rupture of the Se···I interactions. The ion $[PhTeI_4]^-$ of complex **2** did not show any NMR signal, although different windows were inspected for ^{125}Te. An identical result has been already obtained in ^{125}Te NMR experiments of the compound $[PhSe(tu)][PhTeI_4]$ [12]. The assignment of these unexpected results to the electric quadrupole moment of the iodine nucleus (spin 5½) and the lengthy relaxation process of ^{125}Te should be hitherto the only explanation. Unfortunately, we could not go any further experiments because of the limited solubility of the compounds in adequate solvents for low-temperature studies.

3. Experimental

All manipulations were conducted under nitrogen by use of standard Schlenk techniques. Methanol was dried with Mg/I_2 and distilled before use.

3.1. Preparation of $[PhSe(etu)][PhTeBr_4]$ (1)

To 15 mL of a solution of $(PhSe)_2$ (1 mmol, 0.312 g) in methanol, the equimolar amount of Br_2, further 2 mmol (0.204 g) of ethylenethiourea were added {formation of PhSe(etu)Br}. After addition of $PhTeBr_3$ (2 mmol, 0.890 g) the system was softly refluxed under stirring for 2 h. After filtration of the mixture yellow crystals were obtained from the mother solution by slow evaporation of the solvent. Yield: 1.285 g (85%). Melting point: 178–180 °C.

Properties: air stable, gold-yellow crystals. Anal. Calc. for $C_{15}H_{16}Br_4N_2SSeTe$ (782.56): C, 20.64; H, 1.87; N, 3.70. Found: C, 20.57; H, 1.95; N, 3.82%.

^{1}H NMR: 8.64–8.61 (middle, N–H); 7.66–7.31 ppm (m, C–$H_{ar.}$). $^{13}C\{^1H\}$ NMR: 161.12 (C=S), 143.6, 135.7, 130.8, 129.9, 129.4, 128.13, 127.8 ppm ($C_{ar.}$).

IR (KBr): 1555, 1519 [strong, ν_s(C=S]; 3290 cm^{-1} [m, ν_s(N–H)].

3.2. Preparation of $[PhSe(etu)][PhTeI_4]$ (2)

To 15 mL of a solution of $(PhSe)_2$ (1 mmol, 0.312 g) in methanol, the equimolar amount of I_2 was added, turning the color nut-brown. With addition of ethylenethiourea (2 mmol, 0.204 g) the color turned red {formation of PhSe(etu)I}. After addition of $PhTeI_3$ (2 mmol, 1.170 g) the system was softly refluxed under stirring for

2 h. The mixture was filtered and dark-red crystals were obtained from the mother solution by slow evaporation of the solvent. Yield: 1.52 g (83%). Melting point: 149–151 °C.

Properties: air stable, black-reddish crystals. Anal. Calc. for $C_{15}H_{16}I_4N_2SSeTe$ (970.52): C, 18.56; H, 1.66; N, 2.89. Found: C, 18.62; H, 1.71; N, 2.94%.

^1H NMR: 8.55 (m, N–H); 7.67, 7.5–7.2 (m, C–$H_{ar.}$); 4.0, 3.87 ppm (CH_2). $^{13}C\{^1H\}$ NMR: 142.40, 132.9, 131.76, 130.09, 129.93, 129.07, 128.75, 128.54, 127.99 ppm ($C_{ar.}$). IR (KBr): 1550 (s), 1430 (weak) [ν_s(C=S]; 3301 cm^{-1} [m, ν_s(N–H)].

3.3. X-ray structural determination

Data were collected with a Bruker APEX II CCD area-detector diffractometer and graphite-monochromatized Mo Kα radiation. The structure was solved by direct methods using SHELXS [21]. Subsequent Fourier-difference map analyses yielded the positions of the non-hydrogen atoms. Refinements were carried out with the SHELXL package [21]. All refinements were made by full-matrix least-squares on F^2 with anisotropic displacement parameters for all non-hydrogen atoms. Hydrogen atoms were included in the refinement in calculated positions. Crystal data and more details of the data collection and refinements are contained in Table 1.

Acknowledgment

This work was supported with funds from CNPq/FAPERGS (Brazil).

Appendix A. Supplementary material

CCDC 715971 and 715972 contain the supplementary crystallographic data for this paper. These data can be obtained free of charge from The Cambridge Crystallographic Data Centre via www.ccdc.cam.ac.uk/data_request/cif. Supplementary data associated with this article can be found, in the online version, at doi:10.1016/j.jorganchem.2009.04.009.

References

[1] S. Hauge, K. Maroey, T. Oedegaard, Acta Chem. Scand. Ser. A 42 (1988) 56.
[2] H.M.K.K. Pathirana, J.H. Reibenspies, E.A. Meyers, R.A. Zingaro, Acta Crystallo., Sect. C 47 (1991) 516.
[3] B. Krebs, F.-P. Ahlers, Adv. Inorg. Chem. 35 (1990) 235.
[4] A.K.S. Chauhan, Anamika, A. Kumar, R.C. Srivastava, R.J. Butcher, J. Beckmann, A. Duthie, J. Organomet. Chem. 690 (2005) 1350.
[5] E. Schulz Lang, G. Manzoni de Oliveira, R.M. Fernandes Jr., E.M. Vázquez-López, Inorg. Chem. Commun. 6 (2003) 869.
[6] E. Schulz Lang, G. Manzoni de Oliveira, R.M. Fernandes Jr., E.M. Vázquez-López, Z. Anorg. Allg. Chem. 630 (2004) 717.
[7] R.M. Fernandes Jr., G. Manzoni de Oliveira, E. Schulz Lang, E.M. Vázquez-López, Z. Anorg. Allg. Chem. 630 (2004) 2687.
[8] E. Schulz Lang, G. Manzoni de Oliveira, G.N. Ledesma, Z. Anorg. Allg. Chem. 631 (2005) 1524.
[9] (a) I. Haiduc, J. Zukerman-Schpector, Phosphorus, Sulfur Silicon 171 (2001) 171;
(b) J. Zuckerman-Schpector, I. Haiduc, Cryst. Eng. Commun. 4 (2002) 178.
[10] W.-W. du Mont, C.G. Hrib, New perspectives in sulfur, selenium and tellurium, in: F.A. Devillanova (Ed.), Handbook of Chalcogen Chemistry, RSC Publishing, Cambridge, UK, 2007, p. 833ff.
[11] E. Faoro, G. Manzoni de Oliveira, E. Schulz Lang, J. Organomet. Chem. 691 (2006) 5867.
[12] E. Schulz Lang, G.A. Casagrande, G. Manzoni de Oliveira, G.N. Ledesma, S.S. Lemos, E.E. Castellano, U. Abram, Eur. J. Inorg. Chem. 5 (2006) 958.
[13] G.A. Casagrande, E. Schulz Lang, G. Manzoni de Oliveira, J. Organomet. Chem. 691 (2006) 59.
[14] J. Beckmann, M. Hesse, H. Poleschner, K. Seppelt, Angew. Chem. Int. Ed. 46 (2007) 8277.
[15] A. Bondi, J. Phys. Chem. 68 (1964) 441.
[16] G. Mugesh, H.B. Singh, R.J. Butcher, Tetrahedron: Asymmetry 10 (1999) 237.
[17] F. Cristiani, F. Demartin, F.A. Devillanova, F. Isaia, V. Lippolis, G. Verani, Inorg. Chem. 33 (1994) 6315.
[18] O. Vikane, Acta Chem. Scand. A 29 (1975) 787.
[19] S.M. Godfrey, D.G. Kelly, C.A. McAuliffe, A.G. Mackie, R.G. Pritchard, S.M. Watson, J. Chem. Soc. Chem. Commun. (1991) 1163.
[20] N. Petragnani, Tellurium in Organic Synthesis, Academic Press, San Diego, 1994. p. 153ff.
[21] G.M. Sheldrick, Acta Crystallogr., Sect. A 64 (2008) 112.